Organic & Biomolecular Chemistry

Dynamic Article Links

Cite this: *Org. Biomol. Chem.*, 2011, **9**, 7504

www.rsc.org/obc

PAPER

Monitoring the site-specific incorporation of dual fluorophore-quencher base analogues for target DNA detection by an unnatural base pair system†

Rie Yamashige,[a] Michiko Kimoto,[a,b] Tsuneo Mitsui,[b] Shigeyuki Yokoyama[a,c] and Ichiro Hirao*[a,b]

Received 8th July 2011, Accepted 5th August 2011
DOI: 10.1039/c1ob06118f

We developed intramolecular dual fluorophore-quencher base analogues for site-specific incorporation into DNA by an unnatural base pair replication system. An unnatural base pair between 7-(2-thienyl)-imidazo[4,5-*b*]pyridine (**Ds**) and 2-nitro-4-propynylpyrrole (**Px**) exhibits high fidelity in PCR amplification, and the 2-nitropyrrole moiety of **Px** acts as a quencher. Deoxyribonucleoside triphosphates of **Px** linked with a fluorophore (Cy3, Cy5 or FAM) were chemically synthesized, and the fluorescent properties and the enzymatic incorporation of the fluorophore-linked d**Px**TPs into DNA were examined in PCR amplification. The fluorophore-linked d**Px**TPs were site-specifically incorporated by PCR into DNA, opposite **Ds** in templates, with high selectivity. Furthermore, we found that the fluorescence of the triphosphates was partially quenched, but increased upon their incorporation into DNA. These dual fluorophore-quencher base analogues would be useful for site-specific DNA labeling and for monitoring the amplification products of target nucleic acid molecules with a specific sequence. We have demonstrated the utility of the fluorophore-linked **Px** substrates and the **Ds-Px** pairing in real-time quantitative PCR for target DNA molecule detection.

Introduction

Many fluorescent nucleobase analogues and fluorophore-linked bases have been developed for sensing and diagnostic applications that monitor the fluorescence spectral changes upon interaction with target molecules.[1–4] Most of the systems rely on either the fluorescence intensity changes that occur from the stacking interactions of the fluorophore with adjacent molecules, or the spectral changes by FRET between the first and second fluorophores and quenchers. Recently, intramolecular two-fluorophore-linked nucleobase systems have also been developed, by using exciton-controlled hybridization-sensitive fluorescent oligonucleotides.[5,6] These systems are used for analyses of the enzymatic kinetics and structures of nucleic acid molecules,[7] and for the detection of target nucleic acid sequences using hybridization probes,[3] molecular beacons,[8,9] real-time PCR,[10–13] and signaling aptamers.[14,15] Thus, the further development of a variety of fluorescent nucleobases could expand their applications. In particular, a few reports have described the site-specific enzymatic incorporation of fluorescent nucleobase analogues at a desired position within nucleic acids.[16–21]

Here, we present new fluorescent base analogues, intramolecular dual fluorophore-quencher unnatural bases, which function in replication as a third base pair with its pairing partner, enabling the site-specific enzymatic labeling of DNA molecules. For the expansion of the genetic alphabet, we previously developed an unnatural base pair system, between 7-(2-thienyl)-imidazo[4,5-*b*]-pyridine (**Ds**) and 2-nitro-4-propynylpyrrole (**Px**), which exhibits high fidelity in replication.[21] DNA fragments containing the **Ds-Px** pair can be amplified 10^7-fold after 30 cycles of PCR, with the unnatural base pair retained in 93–97% of the amplified DNA fragments. The selectivity of the **Ds-Px** pairing in PCR is as high as 99.8–99.9% per replication. Furthermore, we found that the 2-nitropyrrole moiety of **Px** acts as a fluorescence quencher.[22] Here, we synthesized several fluorophore-linked **Px** triphosphate derivatives. These fluorophore-linked d**Px**TPs were site-specifically incorporated into DNA, opposite **Ds** in templates, by PCR amplification. In addition, we found that the fluorescence of the fluorophore-linked d**Px**TPs was partially quenched. However, upon their incorporation into a DNA strand, the fluorescence intensity was greatly increased. This fluorescent change can be monitored in nucleic acid production and degradation. Using real-time quantitative PCR (qPCR), we demonstrated the ability of the fluorophore-linked d**Px**TPs and the precise **Ds-Px** pairing to detect nucleic acid targets with specific sequences.

[a]*RIKEN Systems and Structural Biology Center (SSBC), 1-7-22 Suehiro-cho, Tsurumi-ku, Yokohama, Kanagawa 230-0045, Japan. E-mail: ihirao@riken.jp; Fax: (+81) 45-503-9645; Tel: (+81) 45-503-9644*
[b]*TagCyx Biotechnologies, 1-6-126 Suehiro-cho, Tsurumi-ku, Yokohama, Kanagawa 230-0045, Japan*
[c]*Department of Biophysics and Biochemistry, Graduate School of Science, The University of Tokyo, 7-3-1 Hongo, Bunkyo-ku, Tokyo 113-0033, Japan*
† Electronic supplementary information (ESI) available: Chemical syntheses of the fluorophore-linked d**Px**TP and their NMR and MS spectra. Complete real-time qPCR data. See DOI: 10.1039/c1ob06118f

Results and discussion

Chemical synthesis of fluorophore-linked dPxTPs and their fluorescent properties

Fluorophore-linked d**Px**TPs (Cy3-d**Px**TP, Cy5-d**Px**TP, and FAM-d**Px**TP) (Fig. 1) were chemically synthesized by reacting 1-(2-deoxy-β-D-ribofuranosyl)-4-[3-(6-aminohexanamido)-1-propynyl]-2-nitropyrrole 5′-triphosphoric acid (NH_2-d**Px**TP)[21] with the *N*-hydroxysuccinimidyl ester of each fluorophore in DMF at room temperature for 12 h (see Supporting Information†). The products were purified by DEAE-Sephadex column chromatography and C18-HPLC. Each triphosphate was identified by ^{1}H- and ^{31}P-NMR and ESI-MS. The fluorescence of each triphosphate was characterized by an excitation maximum at 552 nm and an emission maximum at 563 nm for Cy3-d**Px**TP; ex.: 651 nm and em.: 660 nm for Cy5-d**Px**TP; and ex.: 496 nm and em.: 521 nm for FAM-d**Px**TP, in 10 mM phosphate buffer (pH 7.0).

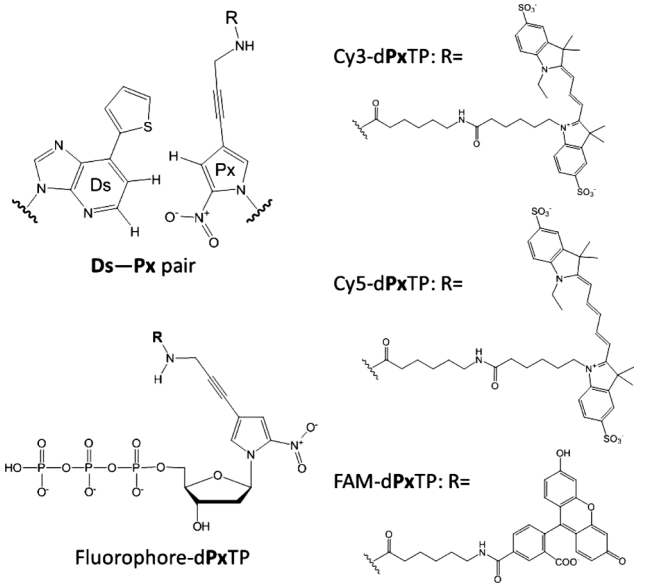

Fig. 1 Chemical structures of the unnatural **Ds-Px** pair and the fluorophore-linked d**Px**TPs.

In the triphosphate synthesis, we found that the fluorescence intensity of each fluorophore-linked d**Px**TP was quenched to some extent, relative to the intrinsic intensity of the fluorophore itself. This partial quenching might be due to the internal stacking between the hydrophobic fluorophore and the 2-nitropyrrole quencher moieties or their intra- and intermolecular statistical collisions in solution. To confirm the involvement of the 2-nitropyrrole moiety in the quenching, we compared the fluorescence intensity change of Cy3-d**Px**TP upon thermal denaturation with that of the ribonucleoside 5′-triphosphate of pyrrole-2-carbaldehyde (**Pa**) linked with Cy3 (Cy3-**Pa**TP). The **Pa** moiety lacks quenching ability. As shown in Fig. 2, the fluorescent intensity of Cy3-d**Px**TP at low temperature was much lower than that of Cy3-**Pa**TP, and both fluorescent intensities approached the same range at high temperature (>80 °C). Thus, Cy3-d**Px**TP was partially quenched by interacting between fluorophore and quencher moieties at low temperature, and its characteristic fluorescence quenching was relieved by the thermal motion.

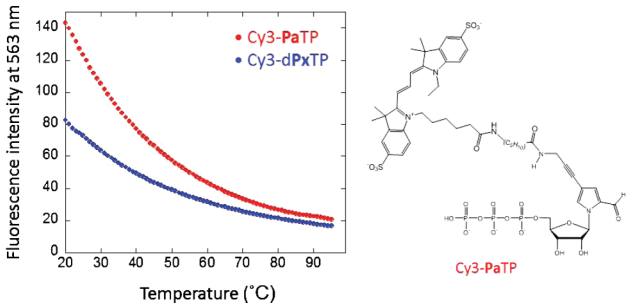

Fig. 2 Temperature dependency of the fluorescence intensities of Cy3-d**Px**TP and Cy3-**Pa**TP. Fluorescence intensities of Cy3-d**Px**TP (blue dots) and Cy3-**Pa**TP (red dots) (1.1 μM each) at 20–95 °C in 10 mM sodium phosphate (pH 7.0), containing 100 mM NaCl and 0.1 mM EDTA. The fluorescence emission (563 nm) of each triphosphate was measured with excitation at 485 nm.

Real-time qPCR using a Ds-containing primer and a fluorophore-linked dPxTP

The partial quenching of fluorophore-linked d**Px**TPs is implicated in the stacking or collision between the fluorophore and **Px** moieties. Thus, we imagined that the fluorophore-quencher interaction would be disturbed when the fluorophore-linked **Px** base was incorporated into a duplex DNA, thus increasing the fluorescence intensity (Fig. 3), which could be monitored by real-time PCR. Therefore, we employed real-time qPCR using the fluorophore-linked d**Px**TP (Cy3-, Cy5- or FAM-d**Px**TP) and a PCR primer tagged with a 3′-**Ds**CGTAATAA-5′ sequence at the 5′-terminus. We examined the effects of the increased sequence length on the **Px** incorporation, and found that the additional sequence of eight natural bases following **Ds** is necessary for the efficient incorporation of **Px** opposite **Ds** (data not shown).

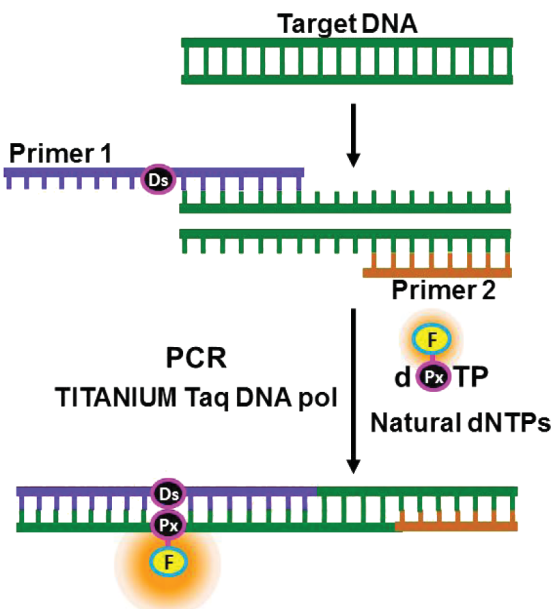

Fig. 3 A real-time qPCR method using the **Ds-Px** pair system with a **Ds**-containing primer and fluorophor-linked d**Px**TP.

Real-time PCR was performed with a 7-log dilution series of a synthetic double-stranded DNA template (98 bp, 3 to 3×10^6

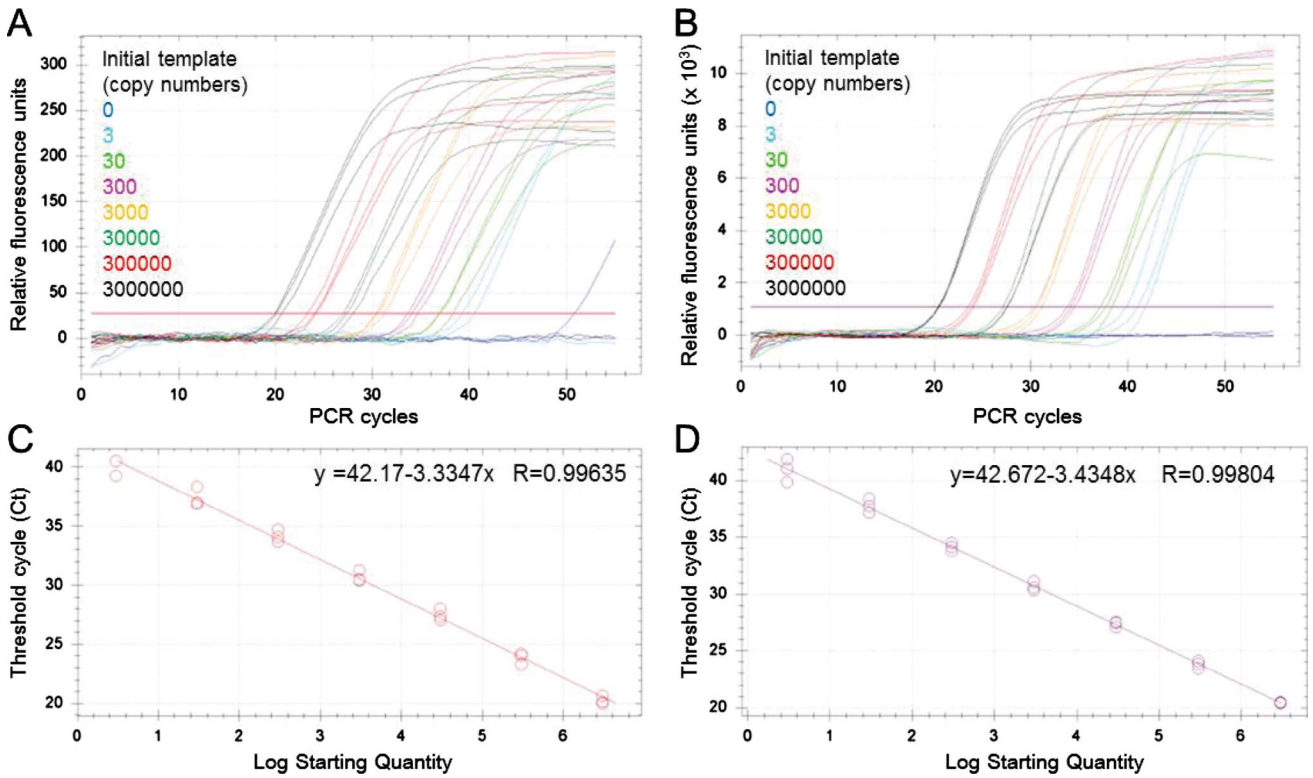

Fig. 4 Amplification plots (A and B) and linear standard curve analysis (C and D) of 10-fold dilution series from 3 to 3×10^6 copies of a 98-bp double-stranded DNA using a **Ds**-containing primer and Cy3-d**Px**TP (A and C) or Cy5-d**Px**TP (B and D). The horizontal red and purple lines in panels A and B indicate thresholds. The cycle threshold values (Ct) obtained from panels A and B were plotted against the log of the template copies.

copies), 2 μM fluorophore-linked d**Px**TP, 200 μM natural dNTPs, 1 μM primers, and TITANIUM Taq DNA polymerase (Fig. 4 and Figures S1–S3 in the Supporting Information†). We employed a two-step cycle, including 94 °C for 5 s and 68 °C for 40 s, and performed 55 cycles of PCR with a CFX96 real-time PCR system (BioRad).

As we expected, as the amplification proceeded, the fluorescence intensity of the fluorophore-linked **Px** was increased by the incorporation of **Px** into the amplified DNA opposite **Ds** in the primer region on the template. Furthermore, high linearity between the cycle threshold (Ct) value and the copy number of the initial DNA fragments was observed in a dynamic range, from 3 to 3×10^6 copies (Fig. 4C and 4D). The Cy3- and Cy5-d**Px**TPs gave clear amplification curves, depending on the number of PCR cycles and the initial DNA concentrations (Fig. 4A and 4B). Only FAM-d**Px**TP fluctuated, in terms of the fluorescence intensity, on both the linear and plateau phases of the amplification, as well as the thermal denaturation curves of the amplified DNA (Figure S3 in the Supporting Information). In particular, the background at lower cycle numbers (fewer than 20 cycles) strongly fluctuated when FAM-d**Px**TP was used. This might be because the interaction between the FAM and 2-nitropyrrole moieties is not very stable or the FAM moiety does not efficiently protrude outside the duplex DNA after the FAM-**Px** incorporation into DNA, thus causing the FAM fluorescence to vary over the PCR cycles. Therefore, the cyanine dyes, such as Cy3 and Cy5, are preferable for this qPCR method.

We also confirmed that Cy3-d**Px**TP was site-specifically incorporated only opposite **Ds**, and almost no Cy3-d**Px**TP was misincorporated opposite the natural bases in the template DNA during PCR amplification. When we performed real-time PCR using primers without **Ds**, no fluorescence change was observed during 55 cycles of PCR in the presence of Cy3-d**Px**TP (Fig. 5A). However, a small amount of Cy5-d**Px**TP misincorporation opposite the natural bases was observed, and the fluorescence was slightly increased during the 55-cycle PCR (Fig. 5B).

Site-specific fluorescent labeling of a DNA fragment during PCR amplification

In this real-time qPCR system, the amplified DNA fragments were site-specifically labeled by the incorporation of the fluorophore-linked **Px** into the amplified products opposite the **Ds** position in the primer. After 55 cycles of PCR of a 7-log dilution series of a 98-bp DNA using a **Ds**-containing primer or its non-**Ds** (control) primer, in the presence of Cy3-d**Px**TP, the amplified DNA fragments were analyzed by gel electrophoresis (Fig. 6). The gel was irradiated at 532 nm to detect the Cy3-containing DNA (Fig. 6A). The total amount of amplified DNA fragments was then observed by conventional SYBR Gold staining (Fig. 6B). Both PCR products obtained from the **Ds** and non-**Ds** primers were observed by the SYBR Gold staining. However, the 532 nm irradiation for Cy3 detected only the amplified DNA fragments from the **Ds**-containing primer. Taken together with data presented above, Cy3-**Px** is site-specifically incorporated opposite **Ds**. This labeling method yields amplified DNA products labeled with the fluorophore at a specific position opposite its PCR primer strand.

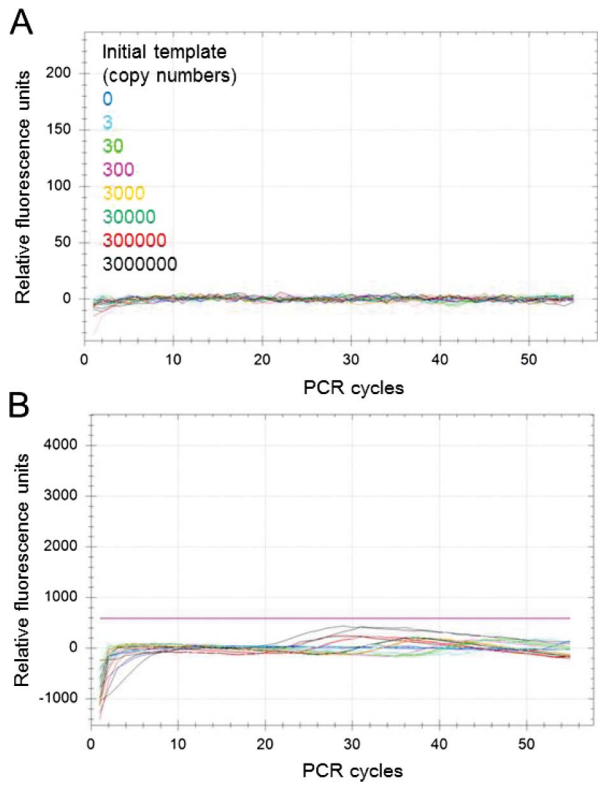

Fig. 5 Amplification plots (A and B) of 10-fold dilution series from 3 to 3×10^6 copies of a 98-bp double-stranded DNA using natural base primers and Cy3-d**Px**TP (A) or Cy5-d**Px**TP (B).

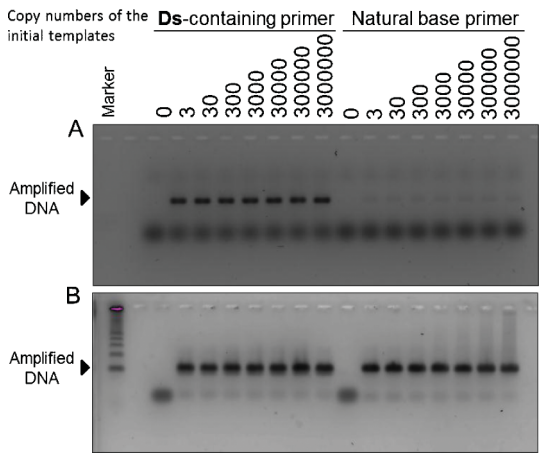

Fig. 6 Agarose gel electrophoresis of 10-fold dilution series from 3 to 3×10^6 copies of a 98-bp double-stranded DNA after 55 cycles of PCR using **Ds**-containing primer or natural base primers with Cy3-d**Px**TP. The Cy3-labeled DNA products were detected by illumination at 532 nm (A), and total amplified DNA products were detected by SYBR Gold staining (B).

Real-time qPCR using a Ds-containing target DNA fragment and Cy3-dPxTP

Next, instead of PCR using the **Ds**-containing primer, we examined the direct detection of target DNA molecules containing one **Ds** base by real-time qPCR, in the presence of Cy3-d**Px**TP and d**Ds**TP (Fig. 7A). For the experiments, we used a single-stranded **Ds**-containing target DNA (55-mer, 0.5 amol–5 fmol) and its primers without **Ds**. In addition, we employed AccuPrime *Pfx* DNA polymerase, instead of TITANIUM Taq DNA polymerase. Although TITANIUM Taq exhibits high efficiency and selectivity for the d**Px**TP incorporation opposite **Ds**, AccuPrime *Pfx* is suitable for enhanced efficiency and selectivity of the complementary **Ds-Px** pairing in PCR. By this real-time method, the Cy3-**Px** incorporation opposite **Ds** in the target could be directly observed by the increased fluorescence changes. As shown in Fig. 7B and 7C, we detected less than an attomole order of the target DNA containing one **Ds** base. We also confirmed that no Cy3-d**Px**TP was incorporated into DNA without **Ds**, under the same PCR conditions (Fig. 7D). Since this system can specifically detect only the **Ds**-containing target DNA, backgrounds caused by primer mishybridization and primer dimer production could be eliminated.

Conclusions

We developed intramolecular dual fluorophore-quencher base analogues, fluorophore-linked d**Px**TPs, for the expansion of the genetic alphabet of DNA. The fluorophore-linked d**Px**TPs were site-specifically incorporated into DNA with high efficiency and selectivity, opposite **Ds** in templates, by PCR. The fluorescence of these modified d**Px**TP substrates was partially quenched, but increased upon their incorporation into DNA. By monitoring the fluorescence changes, the fluorophore-linked **Px** incorporation system could be used for monitoring the production or degradation of target DNA molecules.

We demonstrated the utility of the unnatural fluorophore-linked **Px** and **Ds** pair system in a real-time qPCR method, by using a **Ds**-tag primer and fluorophore-linked d**Px**TP substrates. This real-time qPCR method accommodates conventional PCR primer design: the **Ds**-tag sequence is simply added to the designed primer sequence that is suitable for each target DNA sequence. This simple and specific PCR method can be used in combination with other real-time qPCR methods, such as those employing LUX[10] and Scorpion[11,12] primers, the Plexor system,[16] TaqMan,[13,23] and LightCycler,[24] for the further development of multiplex detection systems.

In addition, after PCR quantification, the amplified products are labeled with Cy3-**Px**, which is useful for further analysis. DNA fragments are usually labeled by PCR amplification with a fluorophore-linked primer. However, our method labels the amplified DNA strands opposite the **Ds**-containing primer. Thus, the combination of our method with fluorophore-fragments can be applied to further experiments, such as FRET between different fluorophores in complementary strands.

Ds-embedded DNA fragments, as shown in Fig. 7, could be employed for DNA authentication and steganography techniques,[21,25,26] such as a security tag like DNA ink. Embedding **Ds** into a security tag DNA could increase the specificity excluding the PCR background problems caused by primer dimer production and by contaminated DNA amplification,[21] as the result of primer mishybridization.

The fluorophore-linked **Px** could also be used for monitoring the degradation or the structural changes of target nucleic acid molecules, which would produce fluorescence intensity changes of the incorporated fluorophore-linked **Px**. For the analyte, DNA and RNA molecules containing the fluorophore-linked **Px** can

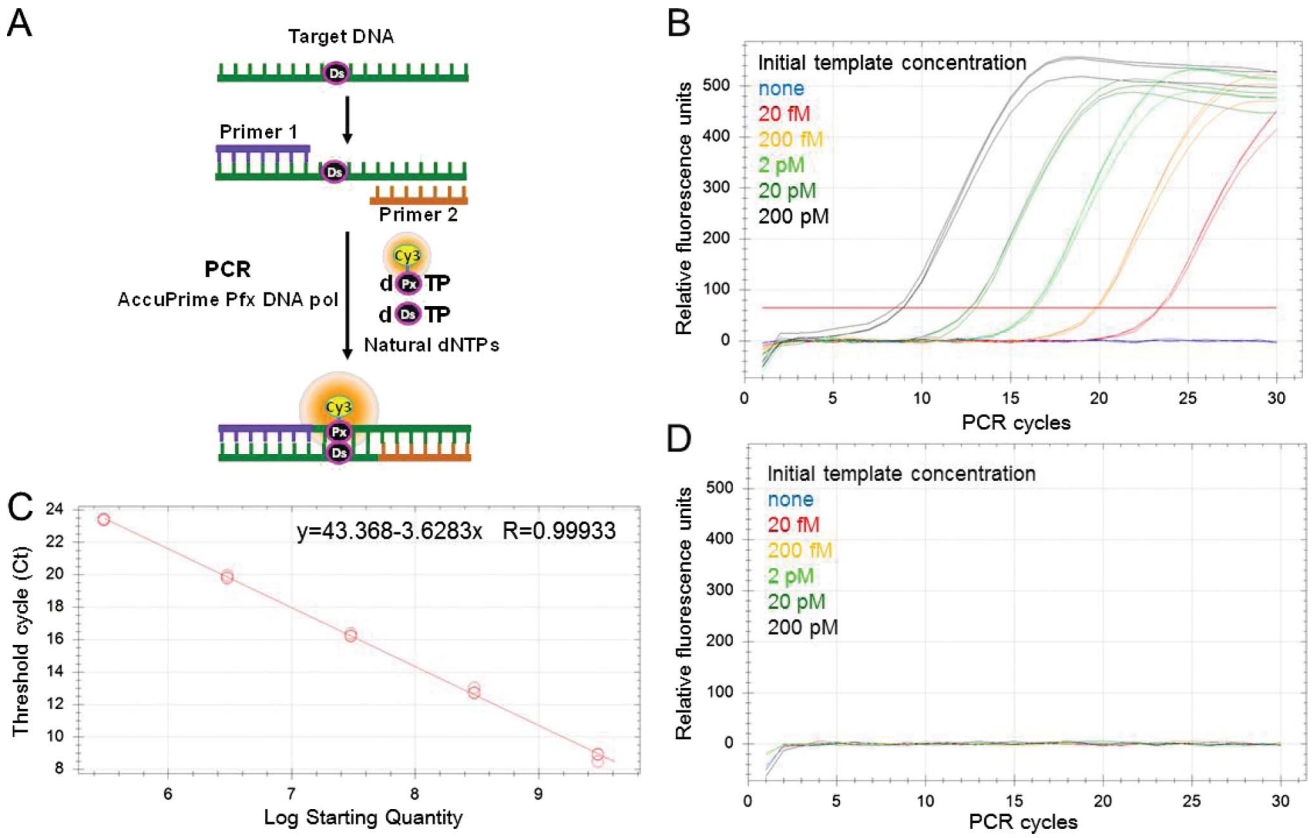

Fig. 7 A qPCR method for a target DNA containing **Ds** (A). Amplification plots (B and D) of 10-fold dilution series from 20 fM to 200 pM of a 55-mer single-stranded DNA containing **Ds** (B) or comprising only the natural bases (D), and linear standard curve analysis (C) for the **Ds**-containing DNA amplification in the presence of d**Ds**TP and Cy3-d**Px**TP. The horizontal red line in panel B indicates a threshold. The cycle threshold values (Ct) obtained from panel B were plotted against the log of the template copies.

be prepared by replication and transcription using **Ds**-containing templates, respectively.

Experimental

Chemical syntheses of Cy3-dPxTP and Cy5-dPxTP

A 0.1 M $NaHCO_3$–Na_2CO_3 solution (pH 8.6, 500 µl) of 1-(2-deoxy-β-D-ribofuranosyl)-4-[3-(6-aminohexanamido)-1-propynyl]-2-nitropyrrole 5′-triphosphoric acid (NH_2-d**Px**TP) (7.6–8.4 µmol) was reacted with Cy3- or Cy5-Mono NHS ester (5.0–6.0 mg, 6 3–7.6 µmol, GE Healthcare) in DMF (300 µl) in the dark at room temperature. After 12 h, 50 mM TEAB (3.0 ml) was added to the reaction mixture. The product (2.7 µmol, 35% for Cy3-d**Px**TP and 3.3 µmol, 52% for Cy5-d**Px**TP) was purified by DEAE Sephadex A-25 column chromatography (1.5 cm × 30 cm, eluted by a linear gradient from 50 mM to 1 M TEAB) and C18 HPLC (eluted by a linear gradient of CH_3CN in 100 mM TEAA, pH 7.0).

Real-time qPCR using a Ds-containing primer and fluorophore-dPxTPs

The PCR reaction (25 µl) was performed in 1 × TITANIUM Taq buffer (Clontech, 40 mM Tricine-KCl (pH 8.0 at 25 °C) containing 16 mM KCl, 3.5 mM $MgCl_2$, and 37.5 µg ml^{-1} BSA) with 0.2 mM of each dNTP (N = A, G, C, and T), 2 µM fluorophore-linked d**Px**TP (Fluorophore = Cy3, Cy5, or FAM), 1 µM Primer1 (29-mer, 5′-AATAATGC**Ds**TCCTCAAAGGTGGTGACTTC-3′ or 5′-AATAATGC**A**TCCTCAAAGGTGGTGACTTC-3′), 1 µM Primer2 (25-mer, 5′-CATGTAGATGCCATCAAAGAAGCTC-3′), TITANIUM Taq polymerase (Clontech) at the manufacturer's recommended concentration (1×), and different concentrations of a 98-bp double-stranded DNA template (copy numbers in each reaction mixture: 0, 3, 30, 300, 3000, 30 000, 300 000 or 3 000 000) on a CFX96 real-time PCR system (BioRad). PCR cycling parameters were 2 min denaturation at 94 °C, followed by 55 cycles of 5 s at 94 °C and 40 s at 68 °C, with an optical read at the end of the elongation step. The detection of each fluorophore with the PCR instrument was accomplished with the appropriate filter sets for excitation: 560–590 nm and emission: 610–650 nm for Cy3; ex.: 620–650 nm and em.: 675–690 nm for Cy5; and ex.: 450–490 nm and em.: 510–530 nm for FAM. The raw data were collected and analyzed by using the CFX Manager v2.0 software. Amplified PCR products were analyzed by agarose gel electrophoresis. An aliquot (4.2 µl) of the reaction mixture was fractionated on a 4% agarose gel. The PCR products on the gel were first detected with an FLA-7000 imager (GE Healthcare) in the Cy3 mode (excitation 532 nm/emission filter O580), and then the DNA fragments on the gel were stained by SYBR Gold (Invitrogen) and detected in the SYBR Green mode (excitation 473 nm/emission filter Y520). The 98-bp double-stranded template was prepared by primer extension,

using two chemically synthesized DNA fragments (60-mer) (5′-CATGTAGATGCCATCAAAGAAGCTCTGAGCCTCCTAA-A-tgacatgcgtgctctggagaac-3′ and (5′-TGGTGACTTC-TACGTCTTCGTACGTCTTCGTTCTTTTCgttctccagagcacgc-atgtca-3′, the complementary regions are shown in lower case). The primer extension (300 µl) was performed in a reaction buffer (10 mM Tris-HCl (pH 7.5) containing 7 mM $MgCl_2$ and 1 mM DTT) with 0.6 mM dNTPs, 3 µM both DNA fragments, and the exonuclease-proficient Klenow fragment (6U, TaKaRa), at 37 °C for 30 min. The products were collected by ethanol precipitation, and the full-length products were purified by electrophoresis on a 10% polyacrylamide gel containing 7 M urea.

Real-time qPCR using a Ds-containing target DNA fragment and Cy3-dPxTP

The PCR reaction (25 µl) was performed in 1 × AccuPrime *Pfx* reaction mix (Invitrogen) supplemented with 0.1 mM dNTPs (final concentration: 0.4 mM each), 0.5 mM $MgSO_4$ (final concentration: 1.5 mM), 2 µM Cy3-d**Px**TP, 25 µM d**Ds**TP, 1 µM Primer3 (40-mer, 5′-CGTTGTAAAA-CGACGGCCAGGATAATACGACTCACTATAG-3′), 1 µM Primer4 (24-mer, 5′-TTTCACACAGGAAACAGCTATGAC-3′), AccuPrime *Pfx* DNA polymerase (1.25 U, Invitrogen), and 55-mer DNA template (5′-TTTCACACAGGAAACAGCTAT-GACGGATC**Ds**TATCCCTATAGTGAGTCGTATTATC-3′ or 5′-TTTCACACAGGAAACAGCTATGACGGTTACCTACCC-TATAGTGAGTCGTATTATC-3′) at different concentrations (final concentrations: 20 fM, 200 fM, 2 pM, 20 pM, and 200 pM). PCR cycling parameters were 30 cycles of 30 s at 94 °C, 30 s at 45 °C, and 2 min at 65 °C, with an optical read at the end of the annealing step (45 °C, 30 s). The data collection and analysis were performed as described above.

Acknowledgements

We thank Akira Sato and Rie Kawai for preparing the nucleoside derivatives. This work was supported by the Targeted Proteins Research Program and the RIKEN Structural Genomics/Proteomics Initiative, the National Project on Protein Structural and Functional Analyses, Ministry of Education, Culture, Sports, Science and Technology of Japan, and by Grants-in-Aid for Scientific Research (KAKENHI 19201046 to I.H., 20710176 to M.K.) from the Ministry of Education, Culture, Sports, Science and Technology of Japan.

Notes and references

1 C. R. Cremo, *Methods Enzymol.*, 2003, **360**, 128–177.
2 J. N. Wilson and E. T. Kool, *Org. Biomol. Chem.*, 2006, **4**, 4265–4274.
3 S. A. E. Marras, *Mol. Biotechnol.*, 2008, **38**, 247–255.
4 R. W. Sinkeldam, N. J. Greco and Y. Tor, *Chem. Rev.*, 2010, **110**, 2579–2619.
5 S. Ikeda, H. Yanagisawa, A. Nakamura, D. O. Wang, M. Yuki and A. Okamoto, *Org. Biomol. Chem.*, 2011, **9**, 4199–4204.
6 A. Okamoto, *Chem. Soc. Rev.*, 2011, DOI: 10.1039/C1CS15025A.
7 S. R. Kirk, N. W. Luedtke and Y. Tor, *Bioorg. Med. Chem.*, 2001, **9**, 2295–2301.
8 S. Tyagi and F. R. Kramer, *Nat. Biotechnol.*, 1996, **14**, 303–308.
9 S. Tyagi, D. P. Bratu and F. R. Kramer, *Nat. Biotechnol.*, 1998, **16**, 49–53.
10 I. Nazarenko, B. Lowe, M. Darfler, P. Ikonomi, D. Schuster and A. Rashtchian, *Nucleic Acids Res.*, 2002, **30**, e37.
11 D. Whitcombe, J. Theaker, S. P. Guy, T. Brown and S. Little, *Nat. Biotechnol.*, 1999, **17**, 804–807.
12 N. Thelwell, S. Millington, A. Solinas, J. Booth and T. Brown, *Nucleic Acids Res.*, 2000, **28**, 3752–3761.
13 P. M. Holland, R. D. Abramson, R. Watson and D. H. Gelfand, *Proc. Natl. Acad. Sci. U. S. A.*, 1991, **88**, 7276–7280.
14 R. Nutiu and Y. Li, *Chem.–Eur. J.*, 2004, **10**, 1868–1876.
15 R. Nutiu and Y. Li, *J. Am. Chem. Soc.*, 2003, **125**, 4771–4778.
16 C. B. Sherrill, D. J. Marshall, M. J. Moser, C. A. Larsen, L. Daude-Snow, S. Jurczyk, G. Shapiro and J. R. Prudent, *J. Am. Chem. Soc.*, 2004, **126**, 4550–4556.
17 M. Kimoto, T. Mitsui, S. Yokoyama and I. Hirao, *J. Am. Chem. Soc.*, 2010, **132**, 4988–4989.
18 Y. Hikida, M. Kimoto, S. Yokoyama and I. Hirao, *Nat. Protoc.*, 2010, **5**, 1312–1323.
19 M. Kimoto, T. Mitsui, Y. Harada, A. Sato, S. Yokoyama and I. Hirao, *Nucleic Acids Res.*, 2007, **35**, 5360–5369.
20 R. Kawai, M. Kimoto, S. Ikeda, T. Mitsui, M. Endo, S. Yokoyama and I. Hirao, *J. Am. Chem. Soc.*, 2005, **127**, 17286–17295.
21 M. Kimoto, R. Kawai, T. Mitsui, S. Yokoyama and I. Hirao, *Nucleic Acids Res.*, 2009, **37**, e14.
22 M. Kimoto, T. Mitsui, R. Yamashige, A. Sato, S. Yokoyama and I. Hirao, *J. Am. Chem. Soc.*, 2010, **132**, 15418–15426.
23 K. J. Livak, S. J. Flood, J. Marmaro, W. Giusti and K. Deetz, *PCR Methods Appl.*, 1995, **4**, 357–362.
24 R. A. Cardullo, S. Agrawal, C. Flores, P. C. Zamecnik and D. E. Wolf, *Proc. Natl. Acad. Sci. U. S. A.*, 1988, **85**, 8790–8794.
25 C. T. Clelland, V. Risca and C. Bancroft, *Nature*, 1999, **399**, 533–534.
26 D. Heider and A. Barnekow, *BMC Bioinformatics*, 2007, **8**, 176.